Magnetic structures of the rare-earth borocarbides RB_2C_2 (R=Tb, Dy, Ho, and Er)

J. van Duijn and J. P. Attfield
Department of Chemistry, University of Cambridge, Lensfield Road, Cambridge CB2 1EW, United Kingdom

K. Suzuki
Graduate School of Engineering, Yokohama National University, 79-5 Tokiwadai, Hodogaya-ku, Yokohama 240-8501, Japan
(Received 6 April 2000; revised manuscript received 12 June 2000)

The ordered magnetic structures of the title compounds have been determined from powder neutron diffraction measurements on ^{11}B-enriched samples down to 4 K. The lowest temperature R=Tb, Dy, and Ho magnetic structures all have a (0 0 1/2) propagation vector. TbB_2C_2 is antiferromagnetic, but DyB_2C_2 and HoB_2C_2 have a net ferromagnetic moment resulting from four noncollinear magnetic sublattices that are consistent with either of two models for antiferroquadrupolar ordering of the $4f$ states. ErB_2C_2 has a commensurate two-sublattice antiferromagnetic structure at 4 K. Intermediate magnetic structures are also observed for R=Ho and Er over narrow temperature intervals. These are sinusoidally modulated spin density waves with propagation vectors (0.11, 0.11, 0.04), and (0.11, 0.11, 0), respectively.

INTRODUCTION

Rare earth borocarbides RB_2C_2 (R=Y, La-Lu)[1] are of interest for their electronic and magnetic properties,[2] in particular, a recently discovered antiferroquadrupolar order at an unusually high temperature of T_Q=24.7 K in DyB_2C_2.[3–5] These materials contain planar BC sheets of fused 4- and 8-membered rings with R cations located between the 8-membered rings of successive sheets. It was originally proposed that the B and C atoms are paired in the 8-membered rings,[6] however, two recent neutron diffraction studies of CeB_2C_2 have shown that an alternating arrangement is formed, as shown in Fig. 1.[7] These rare earth borocarbides are metallic conductors and YB_2C_2 and LuB_2C_2 become superconducting below T_c=3.6 K and 2.4 K, respectively.[8] Other RB_2C_2 compounds show magnetic ordering transitions below 30 K and are not superconducting.[2] Following recent evidence for antiferroquadrupolar order in DyB_2C_2 (Refs. 3–5) and HoB_2C_2,[9] we have used high resolution powder neutron diffraction to determine the magnetic structures of these two borocarbides and those of the adjacent rare earth elements Tb and Er. ^{11}B-enriched samples have been used to avoid the strong neutron absorption of ^{10}B in natural boron.

EXPERIMENTAL

Polycrystalline RB_2C_2 (R=Tb, Dy, Ho, Er) samples were prepared by arc-melting 5 g pellets of the powdered elements (99.9% R, submicron 99.999% graphite, 99.1% boron-11) on a water-cooled copper hearth in an argon atmosphere. The samples were remelted several times to improve homogeneity. Preliminary x-ray-diffraction measurements showed all of the samples to be >98% phase pure. Powder neutron diffraction patterns were collected on instrument $D2b$ at the ILL, Grenoble, France. The samples were placed in a sealed vanadium can within a He cryostat. The profile was recorded in the range $2\theta = 0-160°$ with a neutron wavelength of 1.5943 Å for TbB_2C_2, DyB_2C_2, HoB_2C_2 and 2.3985 Å for ErB_2C_2. Rietveld analyses of the neutron diffraction patterns were carried out using the refinement program FULLPROF[10] with a pseudo-Voigt peak shape function and a refined polynomial background function.

The crystal structures of the RB_2C_2 (R=Tb, Dy, Ho, Er) phases were found to be isostructural with tetragonal CeB_2C_2 (Ref. 6) down to 4 K and the refined parameters are listed in Table I. Additional magnetic diffraction peaks are observed at low temperatures in all cases and have been used to determine the magnetic structures described below.

TbB_2C_2

Magnetic measurements have shown that TbB_2C_2 orders antiferromagnetically at T_N=23.5 K.[2] The neutron diffraction pattern at 4 K (Fig. 2) contains intense magnetic Bragg

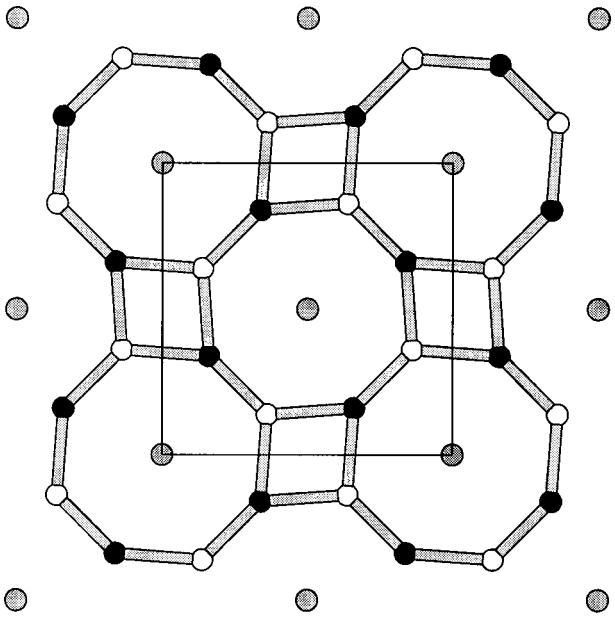

FIG. 1. (001) projection of the RB_2C_2 structure (R/B/C=gray/white/black circles).

TABLE I. Refined structural and magnetic parameters from fits to powder neutron diffraction profiles of RB_2C_2. The crystal structures are tetragonal, space group $P4/mbm$; R on $2(a)$ sites (0,0,0); B and C atoms on $4(h)$ sites $(x, 1/2-x, 1/2)$. The magnetic parameters are the total R moment μ and the net ferromagnetic moment per R atom μ_F, angles θ_1 and θ_2 as defined for models A and B in Fig. 4, the angle between the moments and the c-axis, θ_c, and the independent components of the magnetic propagation vector $(k_x\ k_x\ k_z)$. The weighted profile R-factor and the overall goodness-of-fit parameter are also given.

R	Tb	Dy			Ho			Er	
T (K)	4	4[a]		18.5	4		5.4	4	13.5
a (Å)	5.35481(4)	5.3464(4)		5.34781(8)	5.34076(4)		5.34078(6)	5.33460(4)	5.33619(5)
c (Å)	3.57526(2)	3.54605(5)		3.54790(6)	3.52350(2)		3.52332(4)	3.49425(7)	3.49436(9)
x_B	0.3630(1)			0.3633(3)	0.3630(1)		0.3623(1)	0.3642(4)	0.3632(2)
x_C	0.1613(1)			0.1612(3)	0.1621(1)		0.1613(1)	0.1621(3)	0.1618(2)
Magnetic phase (and model)		(A)	(B)		III(A)	III(B)	IV	II	III
$\mu(\mu_B)$	6.26(1)	8.3(6)	8.2(6)		7.8(1)	7.8(1)	5.97(7)	9.08(4)	7.83(7)
$\mu_F(\mu_B)$	0	2.4(8)	1.8(8)		1.6(1)	1.1(1)	0	0	0
θ_1 (deg)	180	56(8)	41(8)		70.4(8)	48.4(6)			
θ_2 (deg)	180	142(8)	120(8)		134.6(7)	105.6(7)			
θ_c (deg)	90	90	90		72.9(4)	73.1(4)	90	0	0
k_x	0	0	0		0	0	0.1082(4)	0	0.1118(1)
k_z	1/2	1/2	1/2		1/2	1/2	0.0408(5)	0	0
R_{WP} (%)	8.07	39.8	40.0	18.1	8.32	8.23	12.4	11.4	16.3
χ^2	7.62	0.88	0.88	3.11	8.67	8.45	13.6	2.44	2.57

[a]Results are from the fits to the difference between the 4 and 18.5 K profiles.

peaks that are indexed by the (0 0 1/2) propagation vector. The intensities are fitted by a two-sublattice model with moments lying in the xy plane (Table I). The moments are coupled antiferromagnetically to their nearest-neighbors in the [110] and [001] directions. A field-induced ferromagnetic component has been reported for this compound,[2] but this is not observed in the present zero field study.

DyB_2C_2

Previous magnetization, electronic conductivity and specific heat measurements have revealed a ferromagnetic transition at $T_C = 15.0$ K,[2] and a second transition at $T_Q = 24.7$ K which is assigned to long range ordering of the electronic quadrupoles of the Dy^{3+} $4f^9$ states.[3,4,5] The powder neutron diffraction study of DyB_2C_2 was hampered by the moderate sample absorption of natural Dy (for which a correction was applied to the data), and the presence of several weak additional diffraction peaks from an unidentified secondary phase. At 18.5 K, between T_C and T_Q, no lattice distortion or magnetic peaks are evident, and the refined structural parameters are similar to those of the other RB_2C_2 materials (Table I). At 4 K, the appearance of many magnetic peaks evidences a complex magnetic structure (Fig. 3). The magnetic peaks are all indexed by a (0 0 1/2) vector, showing that there are four spins in the basis set. Two models A and B, shown in Fig. 4, can describe the diffracted intensi-

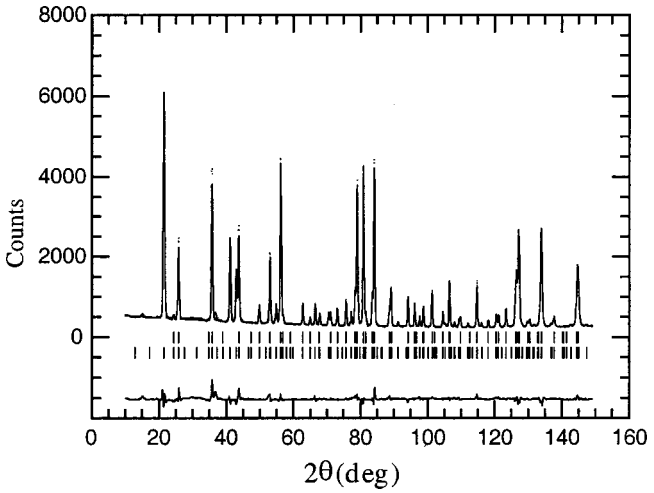

FIG. 2. Fitted neutron diffraction profile for TbB_2C_2 at 4 K. Upper/lower markers correspond to nuclear/magnetic reflections.

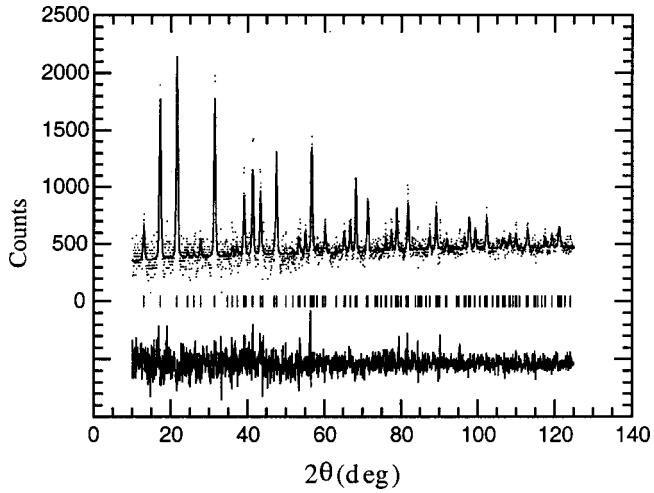

FIG. 3. The fit to the difference between the 4 and 18.5 K profiles of DyB_2C_2.

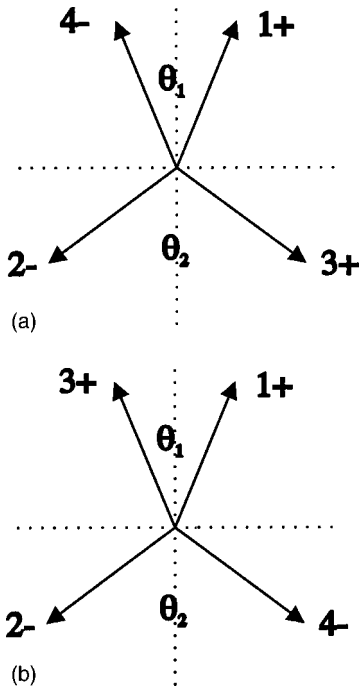

FIG. 4. (001) projections of the alternative magnetic models for DyB_2C_2 and HoB_2C_2-III; (a) model *A* and (b) model *B*. The positions of the *R* spins in the $a\times a\times 2c$ magnetic supercell are 1 (0, 0, 0); 2(1/2, 1/2, 0); 3(0, 0, 1/2) and 4(1/2, 1/2, 1/2). HoB_2C_2 has additional out-of-plane spin components indicated by the + and − symbols; these are absent for DyB_2C_2. The *x* and *y* axes are shown.

ties. These contain four noncollinear sublattices in the *xy* plane, and give equivalent fits when the angles between spins are fixed at $\theta_1=\theta_2=90°$ because of the high crystal symmetry and the powder averaging of diffraction data.

The two magnetic models were fitted to the difference between the 4 and 18.5 K profiles. Refining the θ_1 and θ_2 angles independently leads to magnetic intensities that are slightly inequivalent, but there is no significant difference between the qualities of the two fits as shown in Table I. Both arrangements produce a net moment parallel to the symmetry axes of the arrangements in Fig. 4, which is identified as the [100] direction from the magnetization results of Yamauchi *et al.*, reported during the course of this work.[4] Their spontaneous moment of $2.4\mu_B$ and the saturated moment of $8.5\mu_B$ in the *a*-direction are in good agreement with the values from models *A* and *B*. Both of these arrangements are consistent with antiferroquadrupolar ordering; of spins 1 and 3 in model *A* or of spins 1 and 4 in model *B*, with refined angles between spins $\phi=[180°-(\theta_1+\theta_2)/2]$ of 81(11)° and 100(11)°, respectively. Yamauchi *et al.*[4] have reported a powder neutron fit of model *A*, refined with the constraint $\phi=90°$.

HoB_2C_2

The magnetic phase diagram has recently been determined from magnetization measurements.[9] In zero field, HoB_2C_2 is paramagnetic down to 5.8 K in zero field, magnetically ordered phase IV exists between 5.8 and 5.0 K, and phase III is stable below 5.0 K (magnetic phase labels are taken from Ref. 9). Powder diffraction patterns were recorded at 4.0 and 5.4 K to determine magnetic phases III and IV. The 4.0 K pattern of phase III is comparable to that of DyB_2C_2, and is again indexed by a (0 0 1/2) vector and most of the intensities are fitted by the two models of four sublattices lying in the *xy* plane. However, additional magnetic peaks evidence a further (0 0 0) antiferromagnetic component to the ordering parallel to **c**, as indicated by the +/− symbols in Fig. 4. The two models again give very similar fits to the data with $\chi^2\approx 8.6$ for both [Fig. 5(a)]. The refined net moments are both close to the measured spontaneous magnetization of $1.3\mu_B$ in the [100] direction at 1.5 K,[9] and the angles between the in-plane spin components are $\phi=78(1)$ for model *A* and 103(1) for model *B*. Refining these models with the latter angles constrained to be exactly 90° gave significantly worse fits with $\chi^2\approx 11.7$.

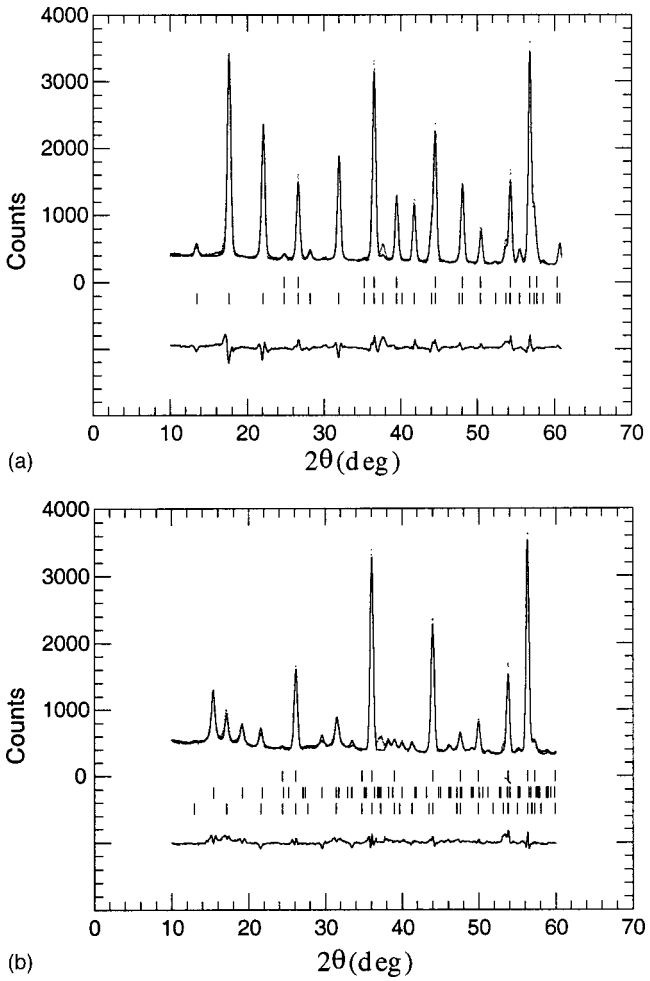

FIG. 5. The low angle region of the fitted neutron diffraction profiles for HoB_2C_2 at (a) 4 K (upper/lower markers for nuclear/magnetic III phases) and (b) 5.4 K (upper/middle/lower markers for nuclear/magnetic IV/magnetic III phases).

The 5.4 K pattern of HoB_2C_2 contains contributions from magnetic phases III and IV. This phase coexistence is in keeping with the first order nature of the transition found by heat capacity measurements. The contribution from phase III was fitted using the above model, and the remaining peaks from phase IV were found to be satellite type reflections, indexed by an incommensurate $(k_x\ k_x\ k_z)$ vector. The intensities of these peaks were fitted by a sinusoidal antiferromagnetic model, in which magnetic moments of sinusoidally

varying amplitude alternate between the [110] and [$\overline{1}\overline{1}0$] orientations, close to the propagation direction. The possibility of an additional component parallel to **c** could not be tested properly because of the presence of such a component in magnetic phase III. The fit to this profile [Fig. 5(b)] is less good than the others reported here, and further variable temperature experiments are needed to confirm the details of the HoB_2C_2-IV magnetic structure.

ErB_2C_2

Magnetization measurements show that zero-field magnetic transitions occur at 13.0 and 14.6 K.[3] Both the intermediate phase III and the low temperature phase II are antiferromagnetic. Figure 6 shows the neutron diffraction profiles at 4, 13.5, and 20 K. Magnetic structure II was determined from the 4 K neutron diffraction pattern. The magnetic peaks are characterized by the (0 0 0) vector and the magnetic structure is a simple, two sublattice arrangement in which the spins at (0,0,0) and (0,0,1/2) in the basic unit cell (Fig. 1) are parallel to **c** and $-$**c**, respectively. The magnetic peaks from ErB_2C_2 at 13.5 K [Fig. 6(b)] are satellites of those observed at 4 K [Fig. 6(a)]. The phase III reflections are indexed by an incommensurate (k_x k_x 0) propagation vector (Table I). The magnetic moments alternate between the **c** and $-$**c** orientations and their magnitudes are sinusoidally modulated with a periodicity of 67.5 Å in the [110] direction.

DISCUSSION

The electronic distribution within these rare earth borocarbides may be written as $R^{3+}(B_2C_2^{2-})e^-$. The $B_2C_2^{2-}$ sheets are isoelectronic with graphite, and the additional electrons partially fill a broad band of borocarbide-π^* and metal-*d* states.[11] The localized $4f^n$ configurations of the R^{3+} ions can thus interact through direct dipolar interactions and by the RKKY (Ruderman-Kittel-Kasuya-Yosida) mechanism through the conduction electrons. Two parallel $(BC)_4$ rings sandwich each R^{3+} ion (Fig. 1) producing a strong crystal field of 4/*m* symmetry which can interact with the magnetic dipole, favoring alignment parallel or perpendicular to **c**, and the electronic quadrupole, depending upon the $4f^n$ configuration.

The variety of magnetic structures found in the RB_2C_2 series for R=Tb to Er reflects variations in the above interactions. For Tb, Dy, and Ho, local anisotropy causes the moments to lie perpendicular to **c**. A simple collinear antiferromagnetic arrangement with propagation vector (0 0 1/2) is found for TbB_2C_2, but in DyB_2C_2 and HoB_2C_2-III, competition between different exchange interactions or exchange and quadrupolar interactions results in four-sublattice arrangements with a net ferromagnetic moment. For ErB_2C_2, the anisotropy causes the moments to lie parallel to **c** which favors a simple two sublattice antiferromagnetic arrangement for the low temperature phase II. HoB_2C_2-III also has an ErB_2C_2-II type antiferromagnetic component so that the moments are tilted by 16° out of the *xy* plane. The *c*-aligned magnetic components in the latter two materials appear to stabilize sinusoidally modulated antiferromagnetic structures over narrow intermediate temperature regions of width 0.8 K for HoB_2C_2 and 1.6 K for ErB_2C_2. These have

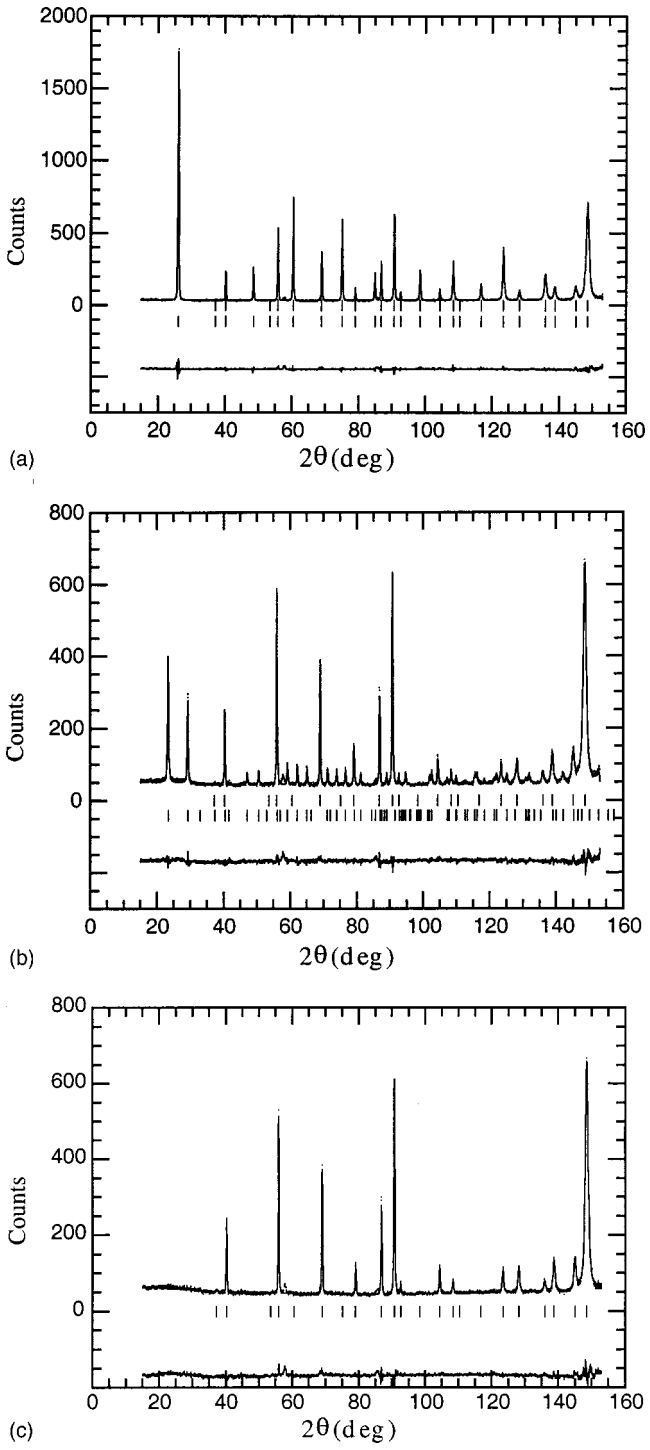

FIG. 6. Fitted neutron diffraction profiles for ErB_2C_2 at (a) 4 K, (b) 13.5 K, and (c) 20 K. Upper/lower markers correspond to nuclear/magnetic reflections.

similar propagation vectors to which the moments are essentially parallel for HoB_2C_2-IV, but perpendicular in ErB_2C_2-III.

Two models consistent with antiferroquadrupolar order are supported by the magnetic diffraction data from DyB_2C_2 and HoB_2C_2-III. Model *A* reflects antiferroquadrupolar order in the *c*-direction, whereas in *B* the order is along the [1/2, 1/2, 1] vector of the structural unit cell. Both of these arrangements are physically plausible as the interacting *R* at-

oms are coordinated to B and C atoms in common (eight for model *A* and two in model *B*) so that the antiferroquadrupolar coupling can propagate by a slight distortion of the BC layers. Model *A* has been proposed in recent studies of DyB_2C_2,[4,5,12] but the possibility of model *B* was not discussed. Our data do not favor one model over the other for DyB_2C_2 and HoB_2C_2-III, and both give interspin angles ϕ that deviate significantly (by $\sim$10°) from the ideal 90° value. This may reflect competition between the quadrupolar and dipolar ordering interactions. Further polarized neutron diffraction experiments on single crystals will be needed to resolve these issues.

ACKNOWLEDGMENTS

We acknowledge EPSRC for provision of neutron beam time at ILL, EPSRC and ICI Katalco for support for JvD and the Ministry of Education, Science, Sports and Culture, Japan, for Grant-in-Aid for Scientific Research on Priority Areas No. 288. We thank Dr. A. Hewat for assistance with neutron data collection.

[1] P. K. Smith and P. W. Gilles, J. Inorg. Nucl. Chem. **29**, 375 (1967); N. A. Fischer and H. A. Eick, J. Inorg. Nucl. Chem. **31**, 891 (1969); J. Bauer and J. Debuigne, C. R. Seances Acad. Sci., Ser. C **274**, 1271 (1972); E. T. Bezruk and L. Ya. Markovskii, Zh. Prikl. Khim. (Moscow) **45**, 3 (1972).

[2] T. Sakai, G. Adachi, and J. Shiokawa, Solid State Commun. **40**, 445 (1981).

[3] H. Yokoyama and K. Suzuki, Meeting Abstr. Phys. Soc. Jpn. **51**, 184 (1996).

[4] H. Yamauchi *et al.*, J. Phys. Soc. Jpn. **68**, 2057 (1999).

[5] K. Hirota, N. Oumi, T. Matsumura, H. Nakao, Y. Murakami, and Y. Endoh, Phys. Rev. Lett. **84**, 2706 (2000).

[6] J. Bauer and O. Bars, Acta Crystallogr., Sect. B: Struct. Crystallogr. Cryst. Chem. **36**, 1540 (1980).

[7] T. Onimaru *et al.*, J. Phys. Soc. Jpn. **68**, 2287 (1999); J. van Duijn, J. P. Attfield, and K. Suzuki, Angew. Chem. Int. Ed. Engl. **39**, 365 (2000).

[8] T. Sakai, G. Adachi, and J. Shiokawa, J. Less-Common Met. **84**, 107 (1982).

[9] H. Onodera, H. Yamauchi, and Y. Yamaguchi, J. Phys. Soc. Jpn. **68**, 2526 (1999).

[10] J. Rodriguez-Carvajal, Physica B **192**, 55 (1993).

[11] J. K. Burdett, E. Canadell, and T. Hughbanks, J. Am. Chem. Soc. **108**, 3971 (1986).

[12] Y. Tanaka, T. Inami, T. Nakamura, H. Yamauchi, H. Onodera, K. Ohoyama, and Y. Yamaguchi, J. Phys.: Condens. Matter **11**, L505 (1999).